EMBELIN ENHANCES THE THERAPEUTIC EFFICACY OF IONIZING RADIATION IN PROSTATE CANCER

Jeffrey DeSano II
University of Michigan
Honors Thesis
Cellular and Molecular Biology
April 2010

Table of Contents

Acknowledgments

I would like to thank Dr. Liang Xu for all of his help, insight, encouragement, and mentorship over the past four years that I have worked in his lab. I am truly grateful for all that he has done for me during my undergraduate collegiate career. His relentless pushing to think critically has given me a greater appreciation for the sciences, especially those related to medicine. I have been truly blessed to have him as my Principle Investigator.

I would like to thank Dr. Lyle Simmons for all of his assistance and his willingness to be my co-sponsor in MCDB. It was his encouragement that made this thesis possible. I sincerely appreciated his kindness and intuitiveness when discussing my research and various projects.

I also would like to thank Yao Dai. He was instrumental in teaching me various assays, helping me interpret the generated data, and aiding me in scientific writing. I appreciated his confidence in me to execute certain experiments on my own. I want to thank Yao for his animal studies work as well as his oversight and execution of various experiments for this project.

I have to thank Yang Meng for her insight and work with the animal studies. She was meticulous in her experiments and always open to answer any questions that I had.

I wish to thank the University of Michigan Comprehensive Cancer Center (UMCCC) Histology Core for the immunohistology study, the UMCCC Unit of Laboratory Animal Medicine for help with animal experiments, and the UMCCC Flow Cytometry Core for flow cytometry analysis.

This study was supported by Department of Defense Prostate Cancer Research Program W81XWH-06-1-0010 (to L. X.), NIH R01 CA121830-01 and R21 CA128220-01 (to L. X.), and by NIH through a University of Michigan Cancer Center Support Grant (5 P30 CA46592).

ABSTRACT:

Embelin is a traditional herbal medicine that exhibits anti-tumor effects in human prostate cancer cell lines. However, the combination therapeutic effect of embelin with conventional radiation therapy is not yet determined. In this study, we evaluated the sensitizing potential of embelin with ionizing radiation (IR) in the treatment of PC3 prostate cancer. *In vitro*, embelin combined with radiation treatment potently suppressed PC3 cell proliferation due to enhanced S and G2/M arrest. Furthermore, the combination treatment increased caspase-independent apoptosis. Clonogenic survival assay showed that S-phase arrest by embelin was required for its radiosensitivity. Moreover, such sensitivity was schedule-dependent, demonstrating that the cell cycle not DNA damage repair plays a role in embelin-mediated radiosensitization. In PC3 xenograft model, embelin significantly improved tumor response to X-ray radiation. Combination therapy produced enhanced tumor growth delay and prolonged time to progression, with minimal systemic toxicity. Immunohistochemistry studies showed that embelin plus IR significantly inhibited cell proliferation, induced apoptosis, and decreased microvessel density in tumors as compared with either treatment alone, suggesting an enhanced combinatorial efficacy on tumor suppression and angiogenesis. Our results show that embelin significantly enhances the anti-tumor activity of conventional radiation therapy both *in vitro* and *in vivo*, representing a promising new adjuvant regime for the treatment of hormone refractory prostate cancer.

Introduction

There is a special equilibrium taking place in all organisms. A fine-tuned balance between cell division and cell death is of paramount significance for the development and maintenance of multicellular organisms (1). This balance is governed by a series of macro-molecular events that are termed the cell cycle. There are four main phases of the cell cycle. Cells grow in size and generate RNAs and proteins required for DNA synthesis during the G_1 phase (2). The cell's DNA is then replicated in the S phase (2). At the end of the S phase, the cells enter the G_2 phase, which involves chromatid formation and continued protein synthesis (2). The final phase of the cell cycle is the M phase where cell division occurs (2). Mutations and disorders in these cell cycle processes can have devastating effects like the onset of diseases or development of cancers.

For this reason, understanding the cell cycle is essential to medical researchers. In the field of oncology, the cell cycle is vital to controlling tumor growth because its regulation of cell division and proliferation. The cell cycle even includes various checkpoints that operate as surveillance mechanisms to ensure that the transition from the different cell cycle phases are not initiated until the previous process has been completed (2). Some important checkpoints include the initiation of the S phase (G_1 checkpoint) as well as after the S phase (G_2 checkpoint) (2). In order to proliferate, cancer cells cannot afford to have this checkpoints stop DNA replication and cell division. Thus, the ability to induce cell cycle arrest would hold great potential as a treatment for tumor control because it would not allow the cancer cells to pass the various checkpoints and subsequently divide and multiply.

In addition to halting cell division, cell cycle arrest can force cells to die through programmed cell death. Over the years, programmed cell death has become synonymous with

apoptosis, a cell death process that is characterized by morphological changes and the activation of caspases (1). Yet, increasing evidence suggests that programmed cell death can occur with complete absence of caspase activation (1, 3). Autophagy, characterized by the sequestration of cytoplasm and organelles in autophagic vesicles to the cell's lysosomal system for subsequent degradation, has been distinguished (1, 4). Necrosis, a more chaotic process that involves cellular edema and disruption of the plasma membrane leading to the subsequent release of cellular components, has also been characterized (1, 5). Thus, cell death can occur in a programmed fashion that is independent of caspase activation.

Nonetheless, apoptosis is a form of programmed cell death that has been a central focus of recent research because of its many implications in cancer formation and progression. Defects in the apoptosis machinery have been connected to the resistance of cancer cells to a wide variety of current anti-cancer drug treatments (6). For this reason, vital apoptosis regulators are attractive new targets for designing new anticancer drugs to overcome apoptosis resistance in cancer cells (7, 8).

In men, prostate cancer is the most common malignancy and also the second leading cause of cancer-related death in the United States (9). For this reason alone, it is an urgent public health problem that needs to be addressed. If diagnosed early, hormone therapy is usually administered (10). This is done to systematically ablate the body's levels of testosterone through the inhibition of androgen receptors, which hopefully will slow or stop the growth/spread of prostate cancer. Yet if the cancer becomes androgen-independent and progresses to a more-advanced hormone-refractory prostate cancer, hormone therapy is inadequate and a subsequent treatment is needed (10). Chemotherapy has historically been used to treat these patients with unimpressive results (11). However, current research is attempting to understand the intricacies

of the disease in hope of elucidating more effective therapies. The use of a combination of chemotherapeutic drugs has demonstrated improved response rates (10). Nevertheless, cancer cells develop a resistance to chemotherapeutic drugs over time.

Along with resistance to drug treatments, cancer cells develop a resistance to ionizing radiation therapy. Ionizing radiation causes DNA damage and initiates cellular recovery mechanisms, which include cell cycle arrest, activation of DNA damage response pathways, and apoptosis (12). Still, due to increased exposure and prolonged lengths of time, cancer cells become resistant to ionizing radiation and continue to proliferate. In hope of improving the efficacy of cancer therapy, radiation therapy in combination with chemotherapeutic agents is being investigated (13). Previous research from our lab has shown that the cancer cells' resistance to radiation therapy can be overcome by using small-molecule treatments (14). We investigated a recently identified proteasome inhibitor, celastrol. The small-molecule drug exhibited antiproliferative effects in cancer cells (15). We were the first to report the use of celastrol combined with ionizing radiation. Celastrol was able to sensitize prostate cancer cells to radiation therapy both *in vitro* and *in vivo* (14). We later elucidated that celastrol accomplished this by impairing the DNA damage processing that is activated by the ionizing radiation treatment (14) and modulating the activity of nuclear factor-kappaB (NF-kappaB) (work not yet published). This suggests that the efficacy of overall cancer therapy can be improved by using small-molecule drugs to sensitize the cancer cells to radiation therapy. This radiosensitization ability is of utmost importance in the field of radiation oncology.

Our current and future search for targets can take a page from our pasts. Traditional herbal medicine is a rich source for modern, molecular target-specific drug discovery (16, 17). Over the years, a great amount of effort has been spent to isolate individual compounds from

traditional herbal medicines. Some of these natural products have been screened for anti-cancer activity. Through computational structure-based screening, embelin was discovered from the Japanese Ardisia herb (16). Embelin was shown to be a small-molecular weight inhibitor that binds to the Baculovirus Inhibitor of apoptosis protein Repeat (BIR) domain of the X-linked inhibitor of apoptosis protein (XIAP) (16). XIAP has been shown to inhibit apoptosis by binding the caspase proteins (18, 19). Previous research has demonstrated that embelin blocks the NF-kappaB signaling pathway, which regulates several genes associated with inflammation, proliferation, carcinogenesis, and apoptosis (20). Thus, embelin is a small-molecule inhibitor of XIAP and represents a promising lead compound for designing a new class of anti-cancer treatments (16).

In this study, we investigated if embelin had the ability to radiosensitize prostate cancer cells and thus improve the therapeutic efficacy of ionizing radiation in prostate cancer. Our findings demonstrate that treatment of embelin in combination with radiation therapy enhanced cell growth inhibition and cell death in prostate cancer *in vitro* and *in vivo*. Embelin represents a small molecule that could have great potential in conjunction with radiation therapy to combat hormone refractory prostate cancer.

Materials and Methods

Reagents and cell culture. Embelin (98%) was purchased from INDOFINE Chemical Company (Hillsborough, NJ) as a powder. The powder was reconstituted in dimethyl sulfoxide (DMSO) and stored as aliquots (with a concentration of 50 mM) at -70°C. Fluorogenic substrates DEVD-AFC and Staurosporin were purchased from BioVision (Mountain View, CA). Anti-poly (ADP-ribose) polymerase (PARP) (F-2) antibody was obtained from Santa Cruz Biotechnology

(Santa Cruz, CA). Anti-XIAP (28) antibody was purchased from BD Biosciences (San Jose, CA). Anti-β-actin (AC-74) antibody was obtained from Sigma (St. Louis, MO). Protease inhibitor cocktail was from Roche (Indianapolis, IN). Other chemicals were from Sigma unless otherwise indicated.

Human prostate cancer cell line PC3 was purchased from American Type Culture Collection. Cells were maintained in RPMI 1640 supplemented with 10% FBS, 100 U/ml penicillin, and 100 μg/ml streptomycin, and incubated in a 5% CO_2 humidified incubator at 37°C. All tissue culture reagents were purchased from Invitrogen (Grand Island, NY).

Cell proliferation and cell death assay. The cell proliferation was addressed by growth curve analysis. Briefly, cells were seeded in a 24-well plate at a density of 2×10^5 cells/well and treated with embelin, IR or in combination in triplicate. Every 24 h for up to 7 days, attached cells were harvested and counted using a Coulter cell counter (Fullerton, CA). Relative cell number was normalized by dividing cell number at various times to the average number of untreated control on the first day (day 0). For cell death analysis, total cells (including both floating and attached cells) were harvested and stained with trypan blue. Percentage of cell viability was calculated by dividing the number of negative-stained cells to total cells. Data were from two independent samples in triplicate. Data were plotted and analyzed by GraphPad Prism 5.0 (San Diego, CA).

Flow cytometry. Annexin V binding assay was employed to detect apoptosis, using an Annexin V-FITC and propidium iodide (PI) staining kit (Roche) according to the manufacturer's instruction. Cells in the lower right quadrant were scored as "early apoptosis" [Annexin V (+) /PI (-)], and in the upper right quadrant were scored as "necrosis/late apoptosis" [Annexin V (+)/PI (+)]. For cell cycle and sub-G_1 analysis, the harvested cells were fixed in 70% ethanol at 4^oC

overnight, then treated with propidium iodide (PI, 50 μg/ml) and RNase A (1 μg/ml) for 30 min. Samples were analyzed by flow cytometry (FACSCalibur, BD Biosciences). Sub-G_1 population was calculated from hypodiploid DNA fluorescent in the cell cycle histogram. Data were analyzed using WinMDI 2.8 software (Purdue University Cytometry Laboratory).

Caspase activation assay. After induction of apoptosis, the cells were resolved in a lysis buffer (BioVision), and whole cell lysates (40 μg) were incubated with a concentration of 20 μM of fluorogenic substrate DEVD-AFC in a reaction buffer (BioVision) containing 5 mM concentrated DTT at 37^{o}C for 1 h. The free fluorosignal generated by proteolytic cleavage of the caspase substrate is proportional to the concentration of activated caspase in the lysates. Proteolytic release of AFC was monitored at λex = 405 nm and λem = 500 nm using a fluorescence microplate reader (BMG, Cary, NC). Fold increase of fluorescence signal was calculated by comparing the normalized signal in each treated sample with that in the untreated control.

Western blot analysis. After exposing cells with various treatments, a whole cell lysate was made by lysing cells in a radioimmunoprecipitation assay (RIPA) lysis buffer [50 mM concentration of Tris-HCl (pH 8.0), 150 mM concentration of NaCl, 0.1% SDS, 1% NP-40, 0.25% Sodium deoxycholate, 1 mM concentration of EDTA, and protease inhibitors]. For xenografted tumor tissue, a homogenizer (Fisher) was used. Total extracted proteins were quantified using Bradford reagent (Bio-Rad, Hercules, CA). Whole cell lysates were resolved by SDS-PAGE (Bio-Rad), electrotransferred to nitrocellulose membranes (Bio-Rad) and probed with respective antibodies.

Clonogenic survival assay. Based on treatment stringency, cells were then seeded in 6-well plate(s) at the desired cell density (200~10,000 cells/well), without exposure to embelin. Cells were then pretreated with various doses of embelin for a desired time course, and then the cells were irradiated with 2 to 8 Gy using 300 kV X-rays (21). The same amount of solvent DMSO was added in control wells as vehicle control. On day 5, 0.5 mL of fetal bovine serum was added to each well. After another 5 to 7 day's culture, the plates were gently washed with PBS and stained with crystal violet (0.1%). Colonies containing over 50 cells were manually counted. For each combination treatment, parallel analyses with each agent alone were also done. The cell survival curves were plotted using a linear-quadratic model, and the mean inactivation dose (area under the cell survival curve) was calculated. Triplicate data of each sample were normalized and the cell survival enhancement ratio was calculated as the ratio of the mean inactivation dose in control divided by the mean inactivation dose in treated cells (21).

Animal study. Female athymic NCr-nu/nu mice (5~6 weeks) were inoculated subcutaneously (s.c.) on both sides of the lower back above the tail with 3×10^6 cells/0.2 ml of PC3 cells. When tumors reached around 100 mm^3, the mice were randomized into 4 groups with 8~10 mice per group and treated daily with (*a*) vehicle control [0.1% carboxymethyl cellulose (CMC)]; (*b*) X-ray radiation at 2 Gy fraction on days 1 to 5 weekly for 2 weeks; (c) embelin via oral gavage (p.o) at a dose of 60 mg/kg on days 1 to 5 weekly for 3 weeks; and (d) X-ray radiation plus embelin. Embelin was dosed 1 h before irradiation. Tumor size and body weight were measured twice a week using a venier caliper. Tumor volume was calculated using the formula: (length × $width^2$)/2. Tumor doubling time was evaluated by monitoring the first day when the tumor volume was twice baseline volume, and characterized by Kaplan-Meier estimate (14). All the

experiments were done according to the protocols approved by University of Michigan Guidelines for Use and Care of Animals.

Histological analysis. Tumor samples were fixed in 4% paraformaldehyde at 4 ^{o}C overnight for paraffin embedding. Besides hematoxylin and eosin (H&E) staining, cell proliferation was tested by Ki67 and proliferating cell nuclear antigen (PCNA) staining, apoptosis was detected by Terminal deoxynucleotidyl Transferase Biotin-dUTP Nick End Labeling (TUNEL) staining using an *in situ* ApopTag kit, and tumor angiogenesis was analyzed by anti-mouse CD31 staining.

Statistical analysis. Two-tailed Student's *t*-test was employed for analyzing both *in vitro* and *in vivo* data. Two-way ANOVA was applied to analyze tumor growth. Mantel-Cox (Log-Rank) test was used for survival analysis. All analysis was performed by GraphPad Prism 5.0. A threshold of $P < 0.05$ was defined as statistically significant.

Results

Combination of Embelin with IR inhibits cell growth and induces cell death. Embelin has been reported to exhibit anti-tumor activity in prostate cancer cells *in vitro* (16). Previous reports have shown that small-molecule treatments may help sensitize cancer cells to radiation therapy (14). To investigate if embelin could work in this manner, we first wanted to monitor if it had any effects on cell proliferation and cell death. We used the human prostate cancer PC3 cell line. Here, we confirm that treatment of embelin alone dose-dependently inhibited PC3 cell growth (Fig.1A,C) and induced PC3 cell death (Fig.1B,C, Table 1). From day 5 post-treatment, 10 μM of embelin exerted significant growth control (>45%), whereas 20 μM of embelin showed drastic cell-killing effect (>60%). Furthermore, embelin plus IR treatment achieved more cell growth

inhibition (P<0.001) and cell death (P<0.05) as compared with either treatment alone after day 2 (Fig.1, Table 1). There is an observed cytotoxic effect but only at a higher dose and longer time. These data suggest that embelin works as a cytostatic rather than a cytotoxic agent because it favors suppressing cell proliferation at lower concentrations. Thus, using embelin, as a small-molecule treatment, in combination with ionizing radiation potently reduced cancer cell proliferation as well as enhanced cancer cell death.

Combination of Embelin with IR induces cell cycle arrest. As embelin plus IR treatment exhibited potent anti-proliferation effect *in vitro*, we further tested the cell cycle distribution in treated cells. While IR induced G2/M arrest, embelin alone treatment triggered S-phase arrest dose-dependently (Fig.2A, Fig.S2A). After 72 h, S-phase cell population showed 2.1±0.8 folds at 10 μM and 3.6±1.1 folds at 20 μM, respectively. In addition, embelin plus IR treatment induced both S and G2/M arrest compared to control (P<0.05) (Fig.2B). This result suggests that treatment of embelin alone, as well as combined with IR, induced cell cycle arrest in PC3 cells.

Combination of Embelin with IR triggers caspase-independent apoptosis. As mentioned above, embelin alone or plus IR exhibited cytotoxic effect (Fig.1B). We then determined whether apoptosis is the form of cell death that is involved in such cytotoxicity. Using flow cytometry, cells were scored as "early apoptosis" [Annexin V (+) /PI (-)] and as "necrosis/late apoptosis" [Annexin V (+)/PI (+)]. In addition, apoptotic cells with fragmented or degraded DNA were seen as cells with hypodiploid DNA content and represented by sub-G_1 populations. The combination treatment barely increased Annexin V+ PI- cell population (Fig. 3A). Rather, the combination treatment enhanced Annexin V+ PI+ population, when compared to either treatment

alone (Fig.3B). This suggests the activation of late apoptosis. Also, embelin plus IR treatment induced more hypodiploid sub-G_1 population than either treatment alone (P<0.05), consistent with the known apoptosis-inducer staurosporin (Fig. 3B). This suggests that apoptosis is playing a role in the cytotoxic effect. Also, interestingly, neither single nor combined treatment showed activated caspase-3 (Fig.3C) or PARP cleavage (Fig.3D), which was inconsistent with staurosporin. Furthermore, neither treatment decreased expression of multiple anti-apoptotic proteins that have been shown to be related with caspases, including bcl-2, bcl-xL, Mcl-1, XIAP and cIAP-1 (Fig.S1). These data demonstrate that embelin combined with IR induces cell apoptosis that is independent of the caspases.

S-phase arrest is required for embelin-mediated radiosensitization. An important issue to tackle in cancer research is understanding how cancer cells become resistant to radiation therapy. To improve the efficacy of cancer therapies, this cancer cell resistance must be overcome. In respect to this, we looked to see if the small-molecule embelin could help achieve a greater therapeutic effect for ionizing radiation. The PC3 prostate cancer cell line offered an outstanding opportunity to study this because of the ideal size and morphology of its formed colonies and relative plating efficiency when treated with embelin (Fig. 4A, C). We have shown that treatment of embelin alone induces S-phase arrest and exerts enhanced apoptosis when combined with IR. We next evaluated whether S-phase arrest is correlated with the radiosensitivity by embelin. We performed many clonogenic assays and utilized different time schedules to achieve the greatest therapeutic effect. The clonogenic assays performed showed that embelin alone treatment minimally inhibited PC3 colony growth below 10 μM (Fig.4A). Thus, a concentration of 10 μM was used for later experiments. After pretreatment for 48 h, embelin sensitized

irradiation-induced clonogenic cell death in a dose-dependent manner (Fig.S2B), showing a similar trend as the well-documented radiosensitizer gemcitabine that also induces S-phase arrest (Fig.S2C). With increased pretreatment time, embelin showed elevated clonogenic cell-killing effect with IR, per the enhancement ratio (Fig.4B). When cells were pretreated with embelin for 72 h, maximum effect was observed even at a lower IR dose of 2 Gy (Fig.4C). This result indicates that enhanced radiosensitization is correlated with increased S-phase arrest induced by embelin in both a dose and time dependent manner. To explore whether radiation-induced DNA repair is also involved in embelin-mediated radiosensitization, we compared two different treatment schedules. Cells pretreated with embelin for 1 h before irradiation followed by 24 h post-irradiation embelin treatment showed less clonogenic survival compared to cells pretreated with embelin for 72h before irradiation ($P<0.01$, Fig.4D). This suggests that cell cycle arrest, not DNA repair, is involved in embelin-mediated radiosensitization. Such speculation is further confirmed by immunostaining of nuclear γH2AX. Indeed, embelin treatment barely impaired IR-induced DNA damage repair (Fig.S3). These data together demonstrate that PC3 cancer cells' resistance to radiation therapy can be overcome using the small-molecule embelin. Therefore, embelin enhances the therapeutic efficacy of ionizing radiation in PC3 prostate cancer *in vitro.*

Embelin potentiates IR-induced tumor regression in PC3 xenografts. All data up to this point has been *in vitro*. To be clinically relevant, we next must see if our *in vitro* results translate into positive *in vivo* results. To evaluate the radiosensitization potential of embelin *in vivo*, we established PC3 xenograft tumor model as described in Materials and Methods section, which was based on previously published manuscript from our lab (14). As shown in Fig. 5A, the

combination therapy inhibited tumor growth more potently than either treatment alone ($P< 0.001$ by two-way ANOVA). At the end of treatment (day 18), median tumor size in the combination group was 60% of IR alone ($P< 0.001$), and 18% of control ($P<0.001$) (Fig. 5B). Notably, the mice body weight loss was less than 15% during the treatment, and rapidly recovered right after the cessation of treatment, suggesting that the accumulated systemic toxicity by either treatment is transient and reversible (Fig. 5C). When monitoring tumor growth of each mouse throughout the experiment, the combination treatment significantly increased tumor-doubling time, with 5~6 folds longer than either treatment alone ($P<0.001$ by Mantel-Cox) (Fig.5D), indicating an improvement of the overall survival. Together, these data demonstrate that embelin with IR enhanced prostate tumor regression and prolonged survival with minor systemic toxicity. These are rather promising and exciting *in vivo* results that validate the use of therapeutic treatments of small-molecule therapies in combination with ionizing radiation to enhance the efficacy of overall cancer therapy.

Combination of Embelin with IR reduces cell proliferation and angiogenesis, and induces apoptosis in vivo. To further confirm the anti-tumor efficacy of the combination treatment, tumor samples were processed for both histological and biological analysis. Ki67 and PCNA staining were used to assess cell proliferation in tumor cell populations, TUNEL staining detected DNA damage and apoptosis, and CD-31 staining identified angiogenesis. Embelin plus IR treatment showed fewer Ki67 and PCNA positive cells, more TUNEL-positive cells and fewer CD31-positive microvessels than either treatment alone (Fig. 6A). These differences were found to be significant after quantification between the combination and IR alone group ($P<0.001$ for Ki67 and PCNA; $P<0.05$ for TUNEL and CD31) (Fig.6B). Consistent with TUNEL staining, the

combination, but neither single treatment, induced PARP cleavage in the tumor tissue (Fig. 6C). Moreover, embelin plus IR dramatically decreased XIAP expression than either embelin or IR alone (Fig.6C). These data demonstrate that combining embelin with irradiation potently suppresses cell proliferation, triggers apoptosis and decreases angiogenesis in tumor tissues.

Discussion

In this study, we demonstrated that embelin, a natural traditional medicine, enhances the therapeutic efficacy against prostate cancer progression by radiation both *in vitro* and *in vivo*. Treatment of embelin combined with radiation achieves increased tumor growth inhibition and apoptosis. Moreover, embelin-induced S-phase arrest is required for its radiosensitivity. These data demonstrate the tangible effect of embelin in combination with radiation and provide a potential mechanism of embelin-mediated radiosensitization. This is a novel report on the combinational use of embelin with ionizing radiation to treat human cancer.

Embelin was able to enhance the therapeutic efficacy of ionizing radiation in prostate cancer *in vitro* and *in vivo* because of its radiosensitization ability (Fig. 4A, B, C). However, we wanted to understand how embelin is orchestrating this radiosensitization effect. Treatment of embelin enhanced cancer cell death when combined with IR (Fig. 1, Fig. 3B, Fig. 5A). While IR induced G2/M arrest, embelin alone treatment triggered S-phase arrest (Fig. 2A, Fig. S2A). Correspondingly, the combinational treatment of embelin plus IR induced cell cycle arrest, specifically S-phase as well as G2/M-phase arrest (Fig. 2B). In addition, we investigated DNA repair as another potential mechanism for its radiosensitization effect. Utilizing different time schedules, embelin was found to have a greater radiosensitization effect when pretreated with the prostate cancer cells instead of embelin treatment after ionizing radiation, which would be the opportune time to work through the impairment of the cancer cells' DNA repair mechanisms

(Fig. 4D). This suggests the importance of cell cycle arrest. We further confirmed that DNA repair was not involved in the radiosensitization effect of embelin by immunostaining of nuclear γH2AX (Fig. S3). These data rule out impairment of DNA repair by embelin as a mechanism for its radiosensitization effect in prostate cancer. Thus, embelin induced cell cycle redistribution to achieve its radiosensitization effect.

We further investigated embelin's induction of cell cycle redistribution and its connection to its radiosensitization. We employed various clonogenic assays with different time schedules to achieve the greatest therapeutic efficacy. After pretreatment for 48 h, embelin radiosensitized prostate cancer cells is a dose-dependent manner (Fig. S2B). This showed a similar trend when compared to gemcitabine (Fig. S2C). Gemcitabine is a well-documented radiosensitizing agent that induces S-phase arrest (22, 23). Embelin induces S-phase arrest in a similar fashion to gemcitabine, suggesting that embelin requires S-phase arrest to mediate radiosensitization in prostate cancer. This was further supported by *in vitro* zapping (Fig. 4B,C) and *in vivo* PCNA staining (Fig. 6A). Thus, S-phase arrest is required for embelin-mediated radiosensitization; however, through our investigation, we were not yet able to elucidate the specific molecular mechanism that embelin works through to induce S-phase arrest and the subsequent radiosensitization. The target molecules remain unclear.

Embelin has been proven to be an XIAP inhibitor. XIAP has been shown to block apoptosis and promote cell survival through its strong stimulation of the NF-kappaB pathway (24). Our first mechanistic hypothesis joined these points. However, our data did not agree with this. The NF-kappaB pathway is activated as part of the response to the DNA damage from the ionizing radiation. However, embelin-induced radiosensitization did not connect with the NF-kappaB pathway throughout our experiments because DNA repair was demonstrated to not

be involved. This provided the possibility that embelin could bind different molecule(s) to mediate the radiosensitization effect. Our data showed that S-phase arrest was required for the radiosensitization. Survivin, is a member protein of the inhibitor of apoptosis (IAP) family like XIAP. Survivin plays a role in apoptosis through blocking caspase activation and a role in the cell cycle regulation in cancer (25). It is possible that embelin may bind survivin instead of XIAP in this situation and induce the cell cycle arrest that mediates the radiosensitization effect in prostate cancer; however, embelin could bind both XIAP and survivin. Another possibility is that embelin binds a molecule or receptor that is not related to the IAP family. In addition, there is substantial cross-talk within signaling pathways and embelin could be involved in multiple pathways in cancer cells that result in the radiosensitization effect seen. Future research in our lab needs to focus on carrying out more mechanism-generating experiments in hope of elucidating the molecules that are targeted by embelin to achieve this radiosensitization effect. These experiments can only help us gain invaluable insight into how to overcome cancer cells' resistance to radiation therapy.

Interestingly, our experiments and investigation uncovered a peculiarity. There was a discrepancy of apoptosis mode by combination treatment. *In vitro*, embelin plus IR treatment induced caspase-independent apoptosis (Fig. 3). There was no activation of caspase-3, PARP cleavage, or decreased expression of anti-apoptotic proteins including XIAP. Yet, there was more hypodiploid sub-G_1 population and enhanced Annexin V+ PI+ population with the combination treatment, suggesting late apoptosis – uniquely a caspase-independent apoptosis. While *in vivo*, combinational treatment of embelin plus IR induced caspase-dependent apoptosis (Fig. 6). There was induction of PARP cleavage and decreased XIAP expression with the combination treatment. Nevertheless, the growth inhibition by embelin plus IR treatment is

consistent between *in vitro* and *in vivo* (Fig. 1, Table 1, Figure 5). This peculiarity is odd and needs to be addressed in the future.

Notwithstanding this strange discrepancy and the lack of a defined mechanism, embelin is a potential traditional medicine that can be used as a modern adjuvant therapy to conventional radiation therapy. Our investigation into embelin's ability to radiosensitize prostate cancer cells revealed strong *in vivo* data. Combinational treatment of embelin plus IR in PC3 xenografts inhibited tumor growth potently, significantly increased tumor-doubling time, exhibited transient and reversible systemic toxicity, and reduced angiogenesis (Fig. 5, 6A,B). These encouraging *in vivo* data corroborate the use of small-molecule therapies in combination with ionizing radiation as therapeutic treatments to enhance the efficacy of overall cancer therapy. Our results show that embelin significantly improves the anti-tumor activity of conventional radiation therapy both *in vitro* and *in vivo*. Therefore, embelin represents a promising complementary treatment for hormone refractory prostate cancer.

Figures

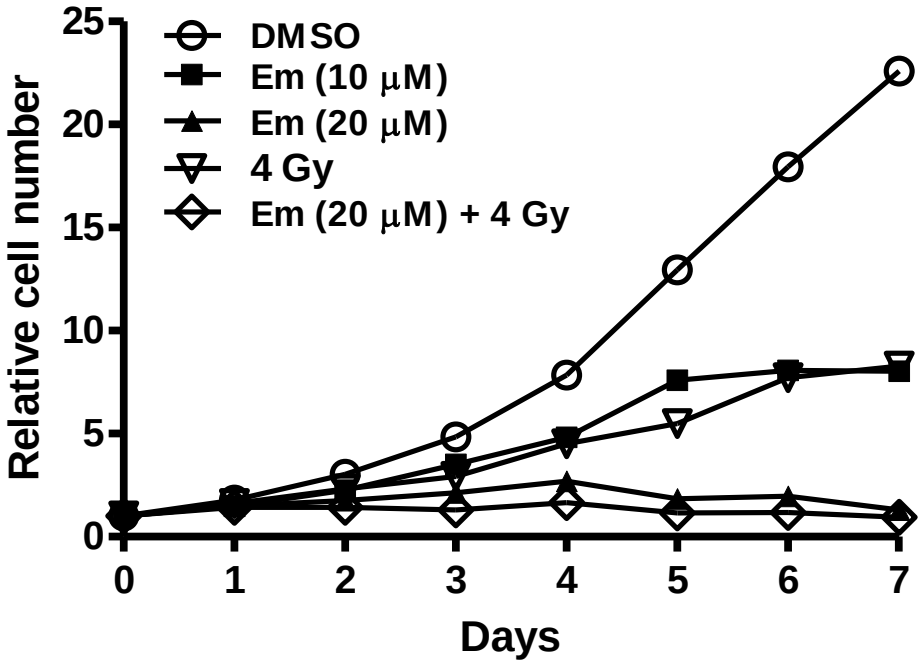

Figure 1A. Treatment of embelin (Em) alone or combined with IR inhibited cell growth. PC3 cells were treated with 10 μM and 20 μM of Em, 4 Gy irradiation, or in combination. Embelin remained continuously exposed to the cells. Attached cells were harvested and counted every day for 7 days. Data are expressed as the ratio of cell number by treatment to the untreated control. Data shown are means ± SD (*n*=6).

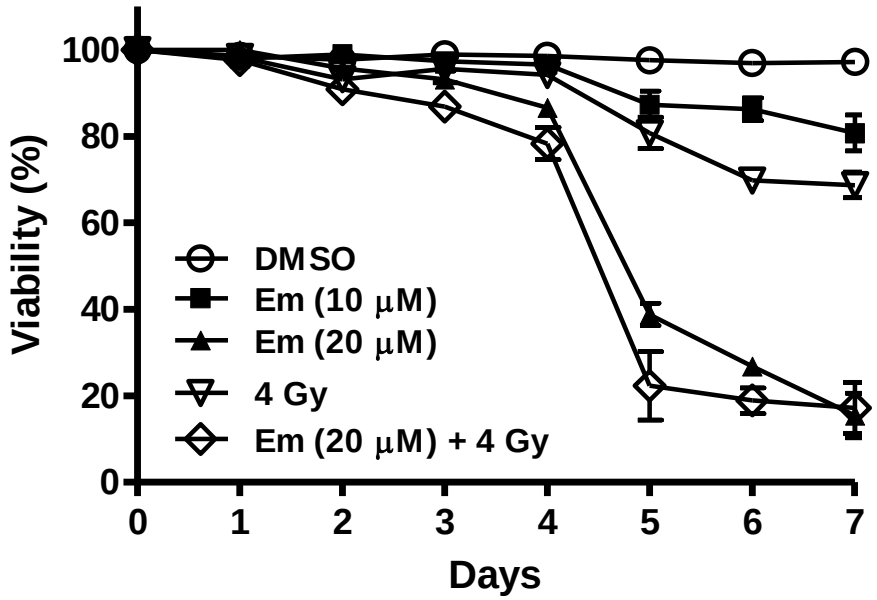

Figure 1B. Treatment of embelin (Em) alone or combined with IR promoted cell death. Both attached and floated cells were harvested for trypan blue staining. Cell viability (%) was quantified by dividing the number of unstained cells to total cells. Data shown are means ± SD (*n*=6).

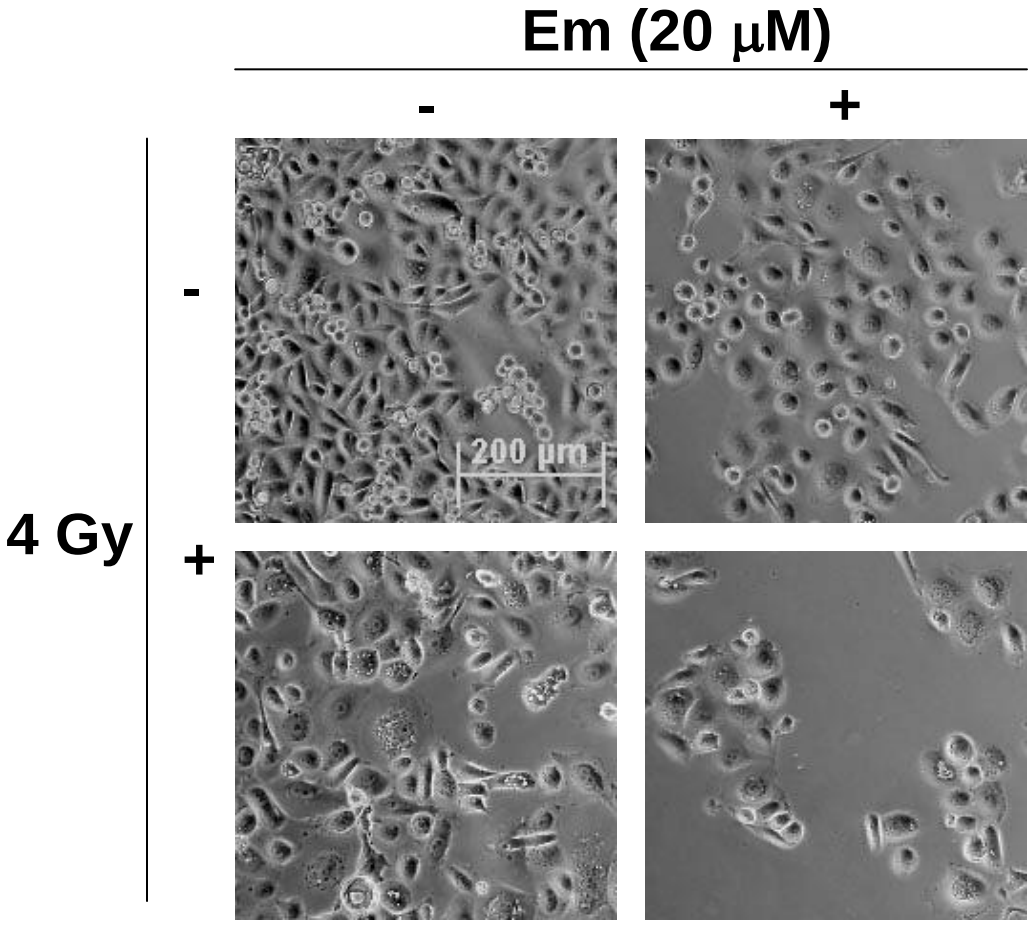

Figure 1C. Treatment of embelin (Em) in combination with ionizing radiation efficiently reduced cell viability. PC3 cell density was monitored 72 h after treatment. Typical pictures were taken in a phase contrast mode. Original magnification, ×100.

Treatment	Cell growth inhibition (%)	Cell death (%)
DMSO	**0.00 ± 1.41**	**1.72 ± 0.60**
Em (10 μM)	**25.18 ± 4.62**	**2.73 ± 1.27**
Em (20 μM)	**54.28 ± 0.94**	**6.80 ± 2.02**
IR (4 Gy)	**39.80 ± 4.77**	**6.13 ± 1.03**
Em (20 μM) + IR (4 Gy)	**72.17 ± 3.56*** **	**14.19 ± 2.94***

Table 1. Effect of treatment of embelin (Em) with IR on PC3 cell growth and cell death. At 72 h after treatment, cell growth inhibition (%) and cell death (%) were calculated based on relative cell number (Fig. 1A) and viability (Fig. 1B), respectively. Data are shown as mean ± SD (n=6) *, P< 0.05; ***, P< 0.001 *vs.* IR or Em alone.

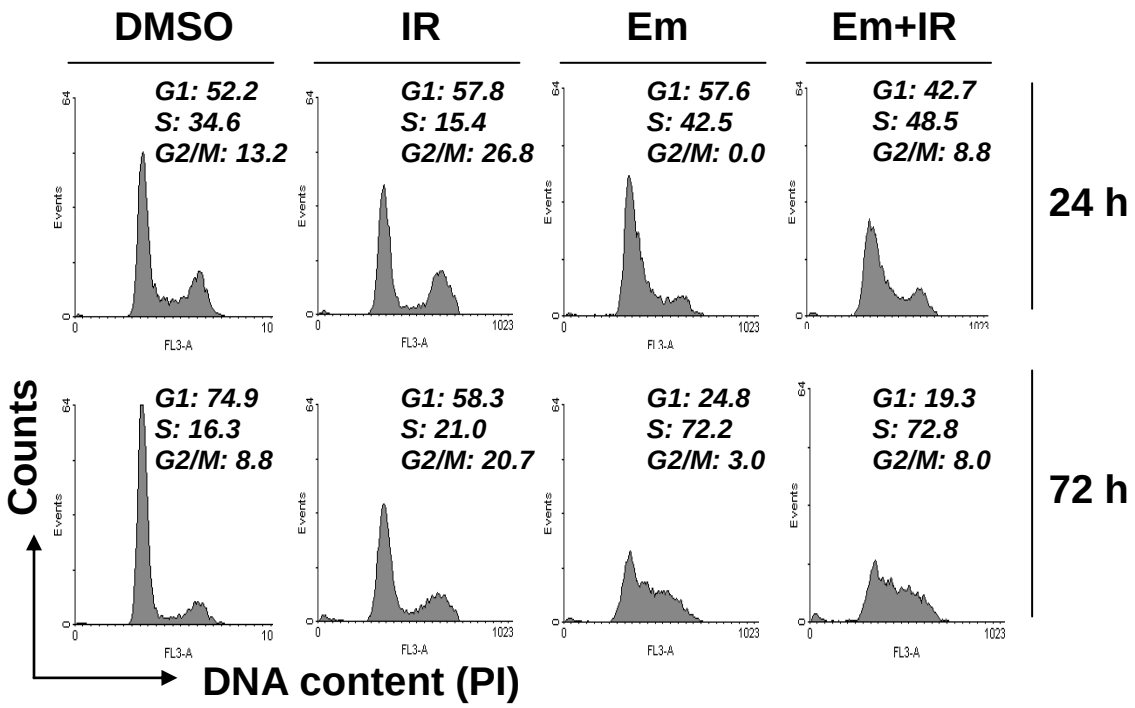

Figure 2A. Cell cycle analysis of PC3 after embelin (Em) and IR treatment. PC3 cells were treated with Em (20 μM), IR (4 Gy) or in combination for 24 h and 72 h, respectively. Data represent one of three independent experiments.

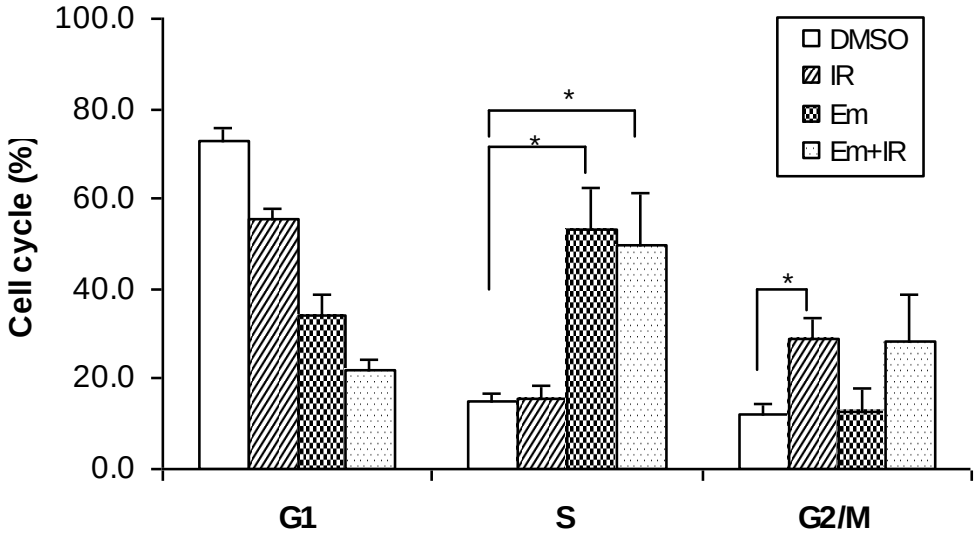

Figure 2B. Quantification of cell cycle analysis. PC3 cell population (%) in each phase was quantified. *Columns*, mean of three independent experiments; *bars*, SD (*n*=3). *, *P*< 0.05.

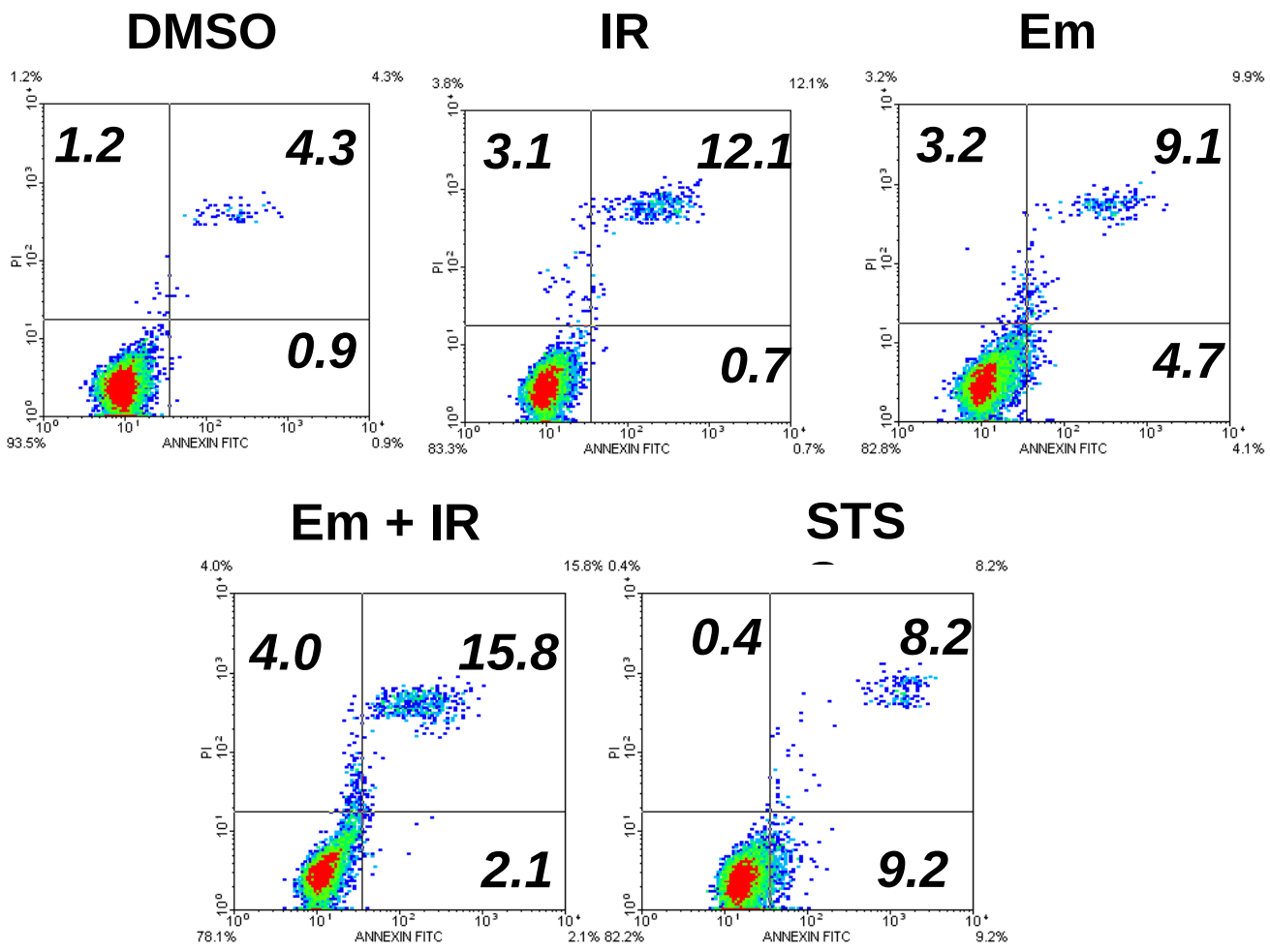

Figure 3A. Combination effect of embelin (Em) and IR on cell death *in vitro*. Cells were treated with Em (20 μM), IR (4 Gy) or in combination for 48 h, or with STS (1 μM) for 4 h. Cells were stained by Annexin V and PI and analyzed by flow cytometry. Cell population in each indicated quadrant is numerically depicted. Data represent one of two independent experiments.

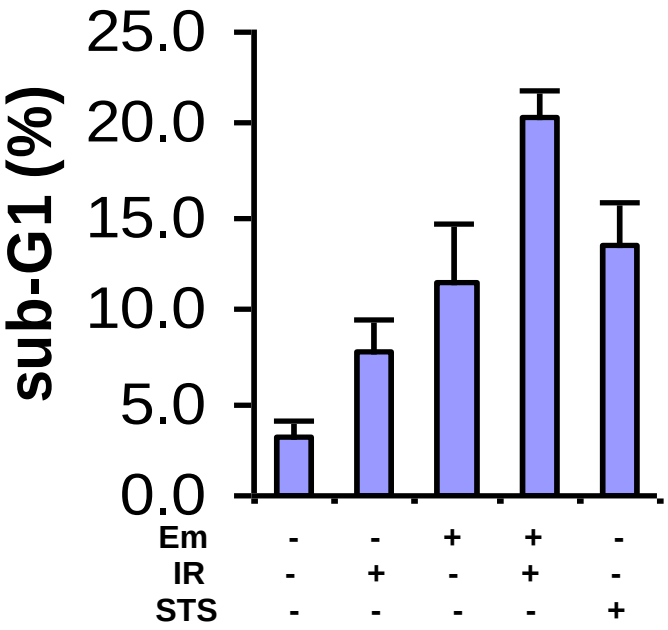

Figure 3B. Treatment of embelin (Em) plus IR enhances sub-G1 population. PC3 cells were treated with Em (20 μM), IR (4 Gy) or in combination for 72 h, or with staurosporin (STS, 1 μM) for 24 h as a positive control. *Columns*, mean of two independent experiments; *bars*, SD (n=2). *, P< 0.05.

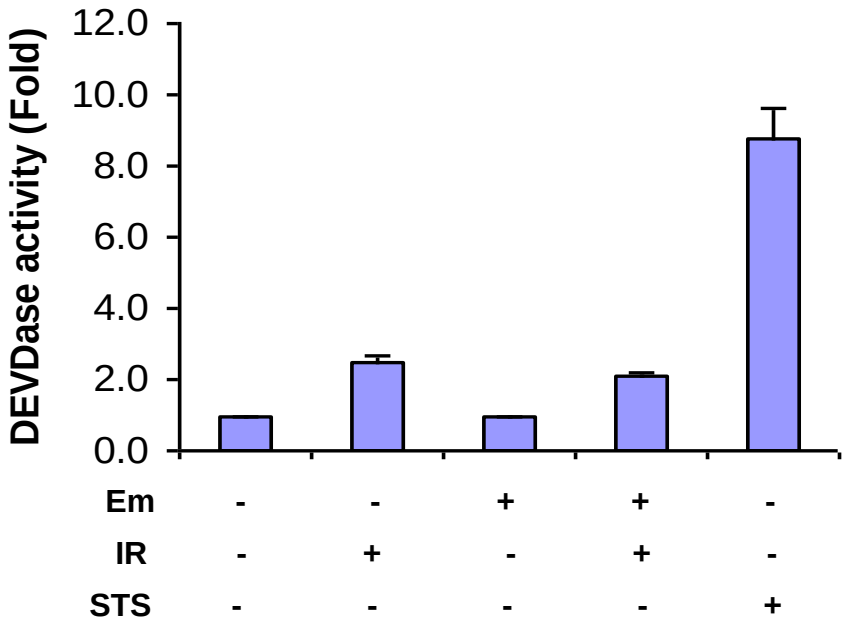

Figure 3C. Treatments of embelin (Em) and IR did not activate caspases. PC3 cells were treated with Em (20 μM), IR (4 Gy) or in combination for 72 h, or with staurosporin (STS, 1 μM) for 24 h as a positive control. Enzymatic activity caspase-3 was determined by fluorescence. *Columns*, mean; *bars*, SD (*n*=3).

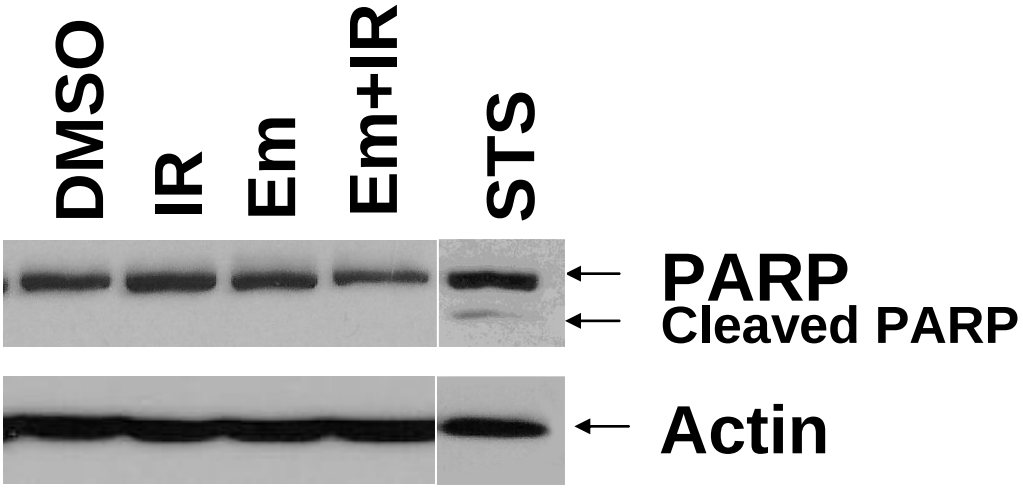

Figure 3D. Treatment of embelin (Em) and IR did not cleave PARP. PC3 cells were treated with Em (20 μM), IR (4 Gy) or in combination for 72 h, or with staurosporin (STS, 1 μM) for 24 h as a positive control. Whole cell lysates (50 μg) were analyzed by Western blot and visualized by anti-PARP antibody. Actin was used as a loading control.

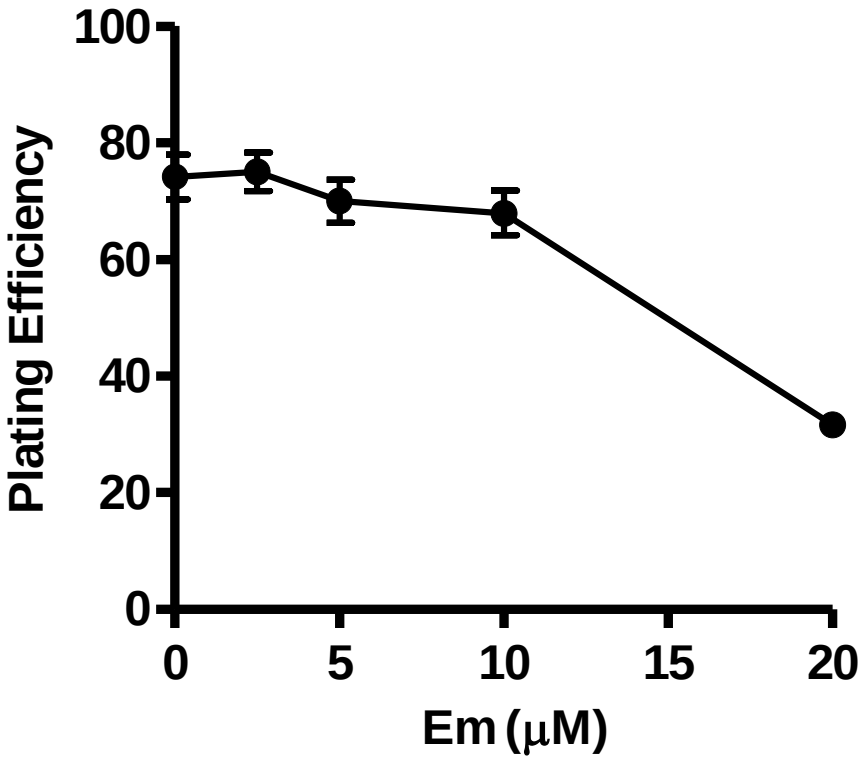

Figure 4A. Relative plating efficiency sows that embelin (Em) treatment alone minimally inhibited colony growth. PC3 cells (200 cell/well) were treated with indicated dose of Em for 72 h and incubated in the fresh medium without Em for another 11 days. Plating efficiency is expressed as a percentage of colonies in treated group by untreated control. *Bars*, SD (*n*=3).

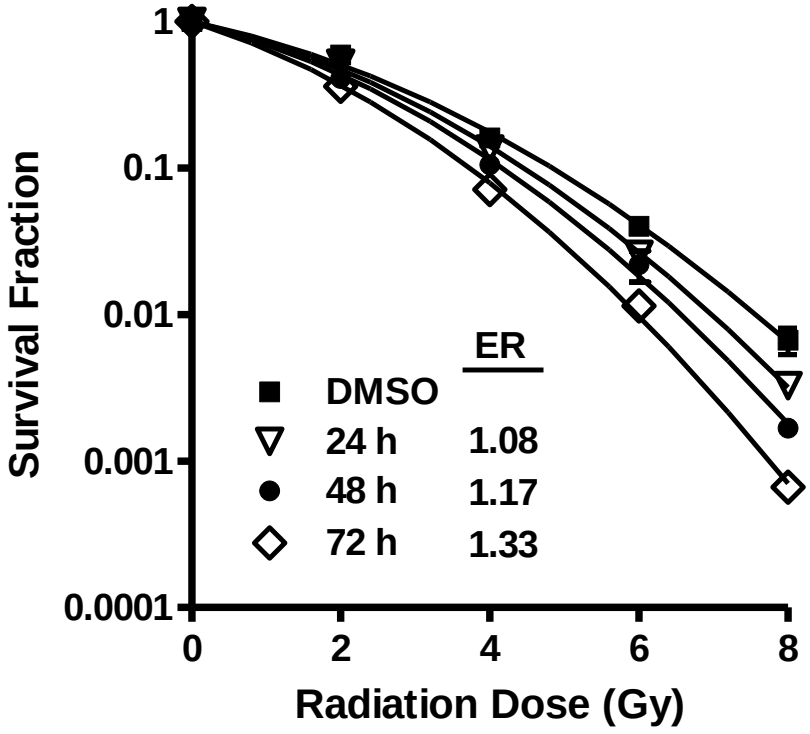

Figure 4B. Radiosensitization effect of embelin (Em). PC3 cells were pretreated with 10 μM of Em for 24 h, 48 h, and 72 h, respectively, and irradiated. Cells were then seeded at desired densities according to different doses of IR without Em. The survival curves were plotted using a standard linear-quadratic model. ER, enhancement ratio. *Bars*, SD (*n*=3). Data represent one of three independent experiments.

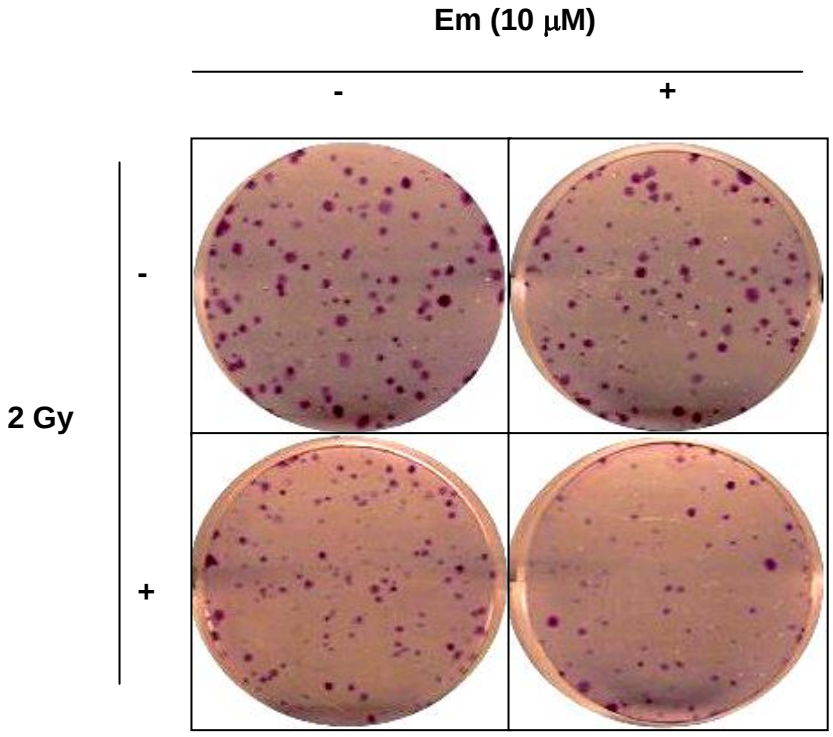

Figure 4C. S-phase arrest is correlated to embelin's (Em) radiosensitization effect. PC3 cells were pretreated with 10 μM of Em for 72 h and irradiated. Cells were then seeded at desired densities according to different doses of IR without Em. Colonies were stained with crystal violet and wells were scanned. Typical wells are shown.

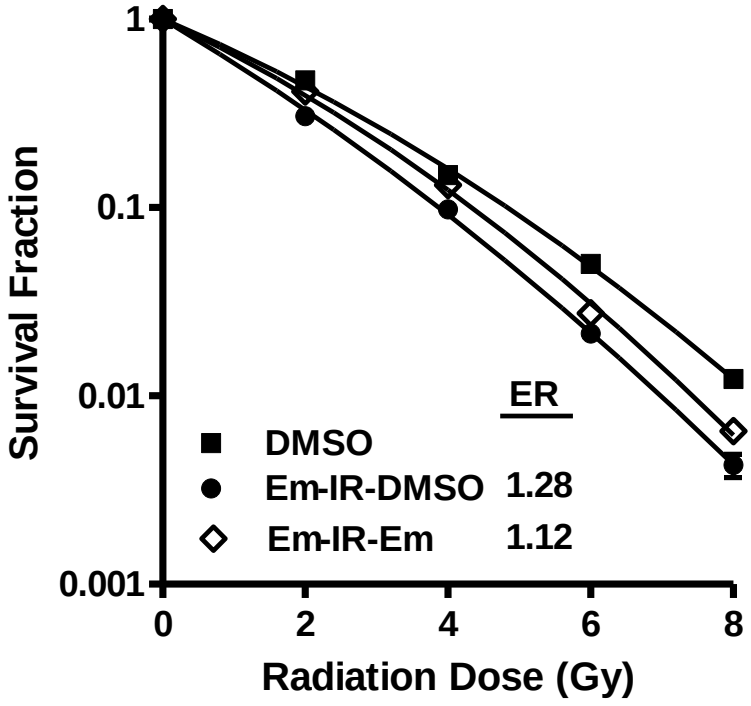

Figure 4D. S-phase arrest, not DNA repair, is required for embelin-mediated radiosensitization. PC3 cells were exposed to Em and IR with two different schedules. *Em-IR-DMSO*: cells were pretreated with 10 μM of Em for 72 h and irradiated. Right after radiation, cells were seeded for clonogenic assay without Em (with DMSO control). *Em-IR-Em*: cells were pretreated with 10 μM of Em for 1 h and irradiated. Cells were incubated with Em (10 μM) for another 24 h post-irradation and seeded. Clonogenic survival analysis was performed as described in *B*. *Bars*, SD (*n*=3). Data represent one of two independent experiments.

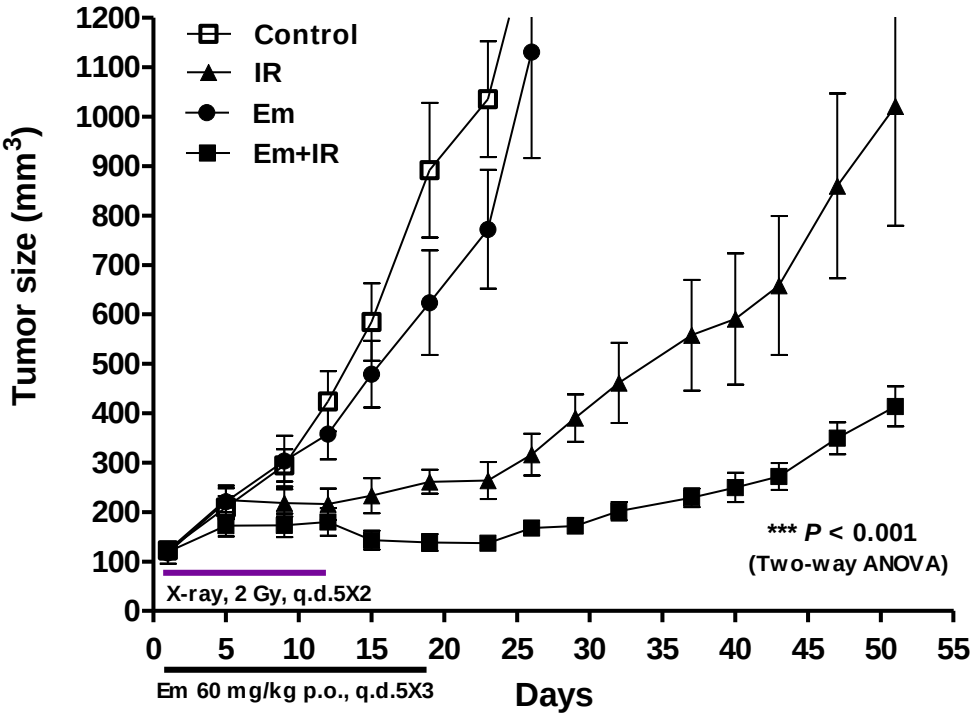

Figure 5A. Tumor growth curve by various treatments. Nude mice bearing PC3 tumors were treated with Em, IR, or in combination, as described in *Materials and Methods*. Tumor size was measured twice a week using a venier caliper. Tumor volume was calculated using the formula: (length × width^2)/2. Data are shown as mean ± SEM (*n≥14*). ***, *P*<0.001 *vs*. IR (two-way ANOVA).

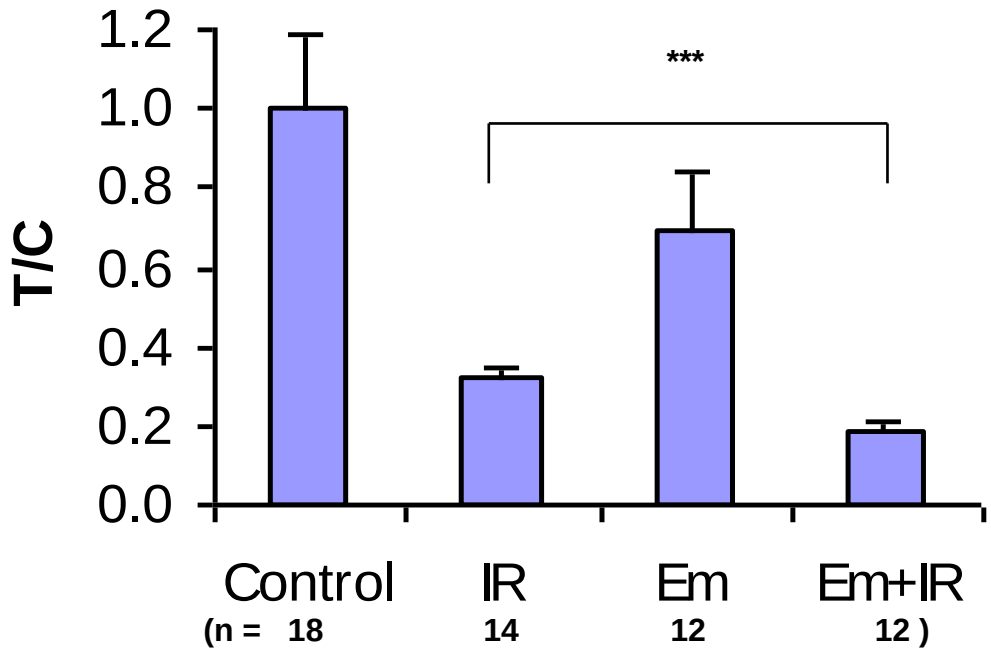

Figure 5B. Combination treatment of embelin (Em) with IR significantly suppressed tumor growth. Tumor suppression (T/C) was calculated as the ratio of median tumor volume in treated group compared with control at the cessation of the treatment (day 18). *Columns*, mean; *bars*, SEM. Tumor number (*n*) of each group is shown. ***, $P<0.001$.

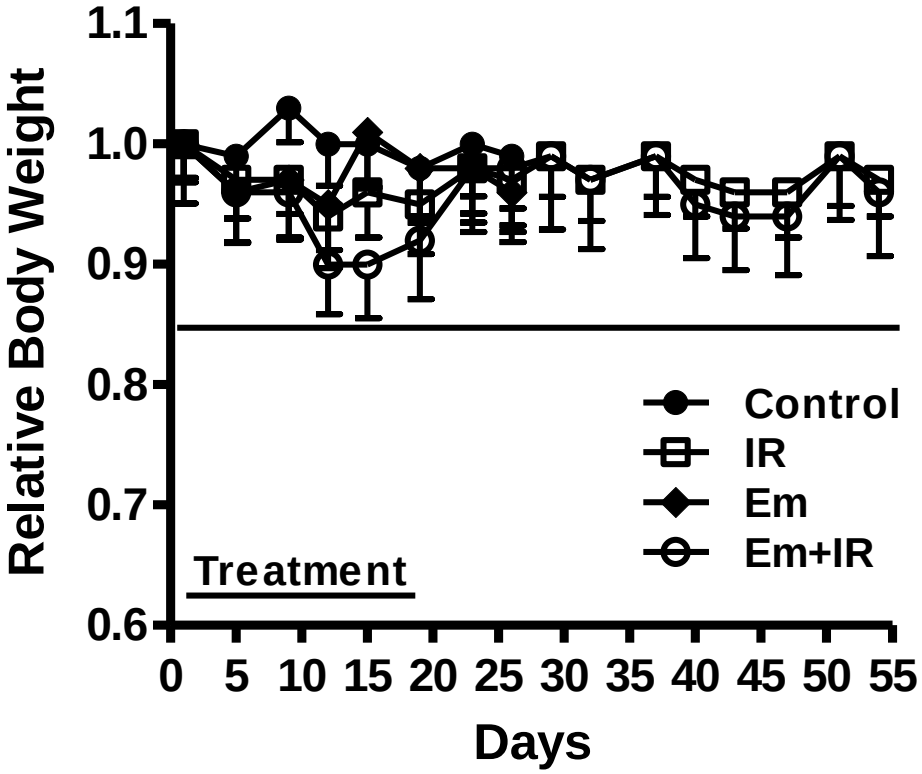

Figure 5C. Treatments' systemic toxicity is transient and reversible. Relative body weight is expressed as the ratio of body weight at various times after treatment compared with the first day of treatment (day 0). Body weight were measured twice a week using a venier caliper. Data are shown as mean ± SEM (*n*=9). Only minus SD bars are shown to simplify the figure. A threshold of "0.85" is set as a solid line to evaluate body weight loss.

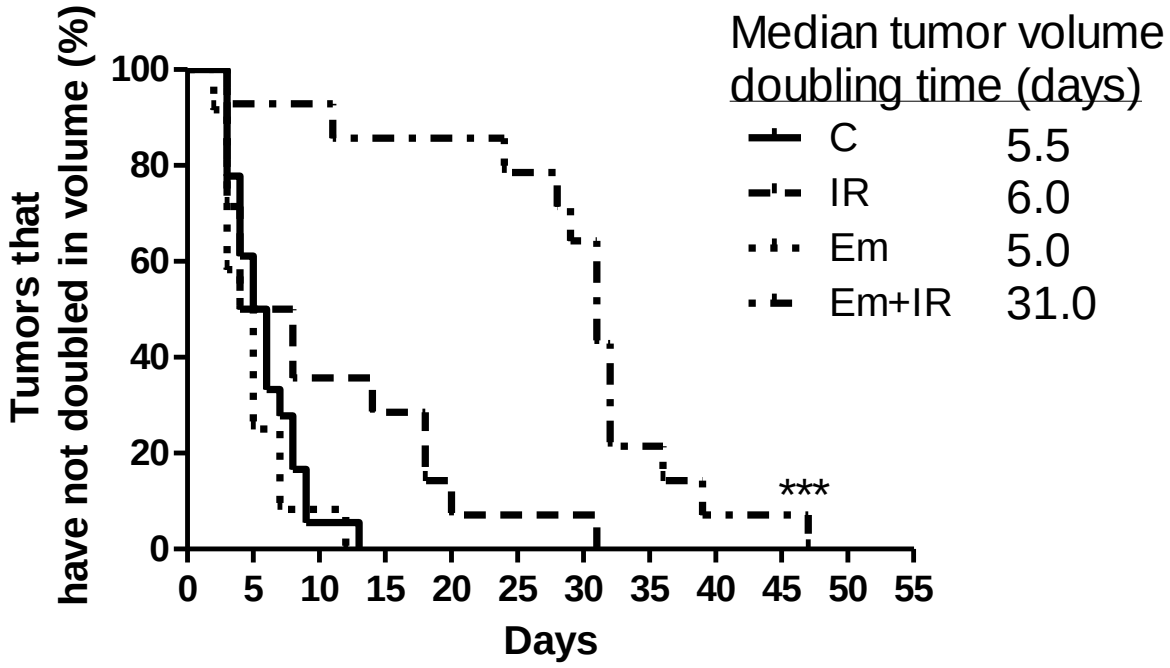

Figure 5D. Combination treatment of embelin (Em) with IR drastically increases tumor doubling time. Tumor doubling time was evaluated by monitoring the first day when the tumor volume was twice baseline volume, and characterized by Kaplan-Meier analysis. The median tumor volume doubling time of each group is depicted numerically. ***, $P<0.001$ *vs*. IR (Mantel-Cox test). Tumor number of each group is described in Figure 5B.

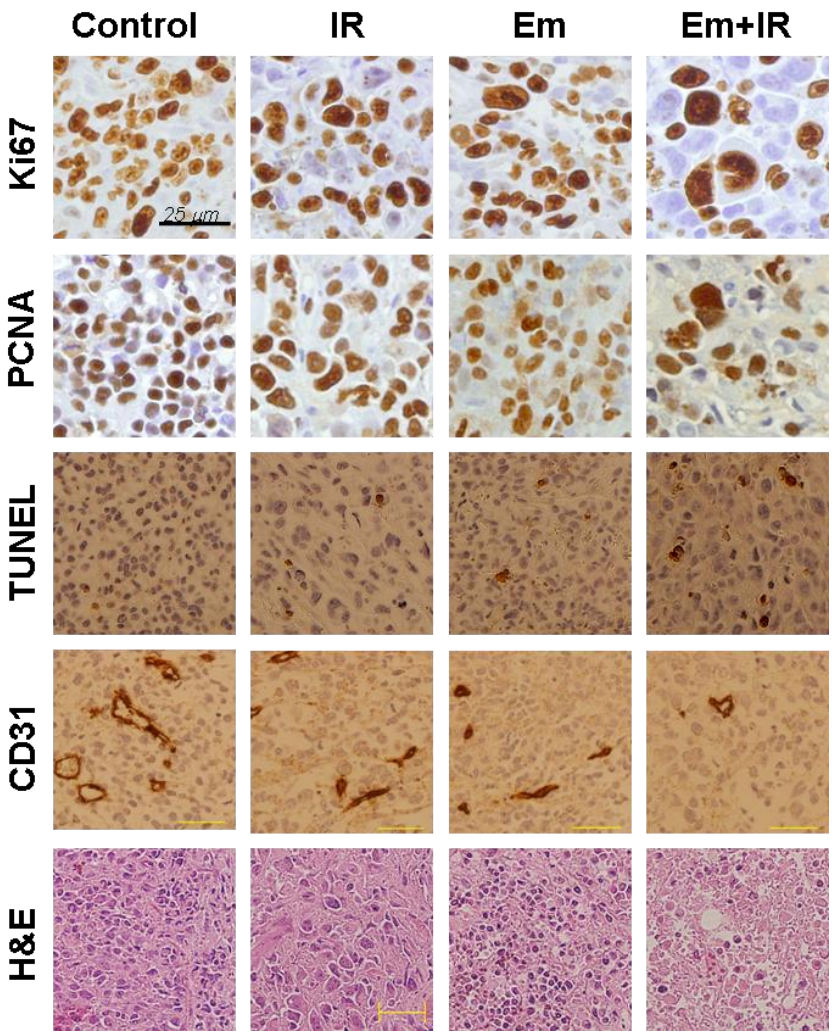

Figure 6A. Immunohistochemistry of tumor tissues shows reduced cell proliferation and angiogenesis and increased apoptosis with combination treatment. Tumor sections were processed by anti-Ki67, anti-PCNA, TUNEL, anti-mouse CD31 and H&E staining. Original magnification, ×400.

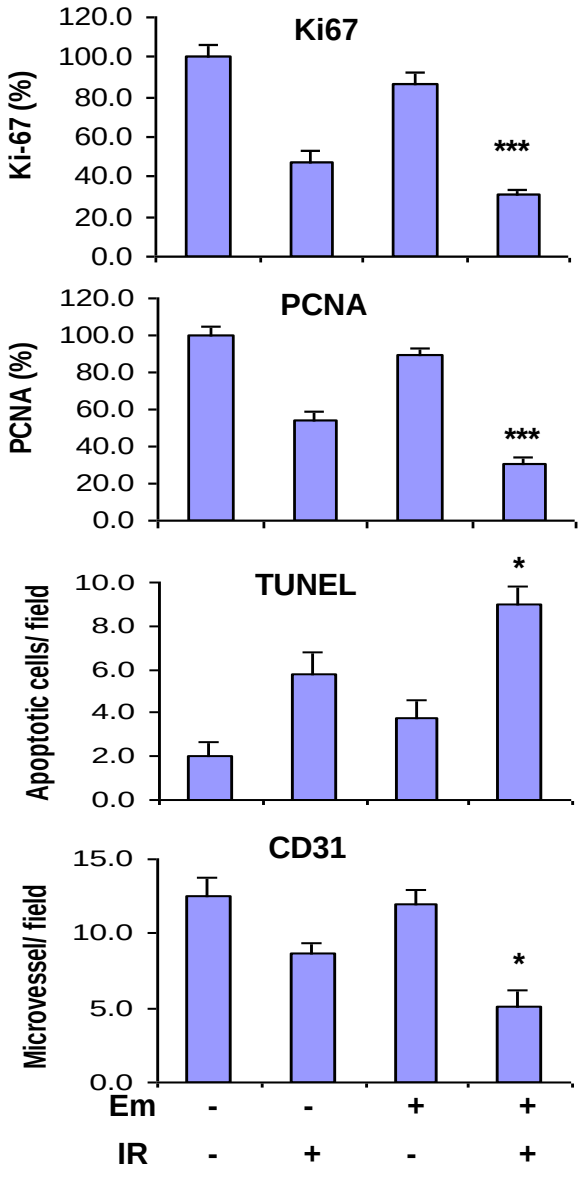

Figure 6B. Quantification of immunohistchemistry analysis in Figure 6A. Positive stained cells or microvessels were quantified by counting 8 random fields. Data are presented as a percentage (for Ki67 and PCNA) or an absolute counting (for TUNEL and CD31) per field (Original magnification, ×200). *Columns*, mean; *bars*, SEM (*n*=8). *, $P< 0.05$; ***, $P< 0.001$ *vs*. IR.

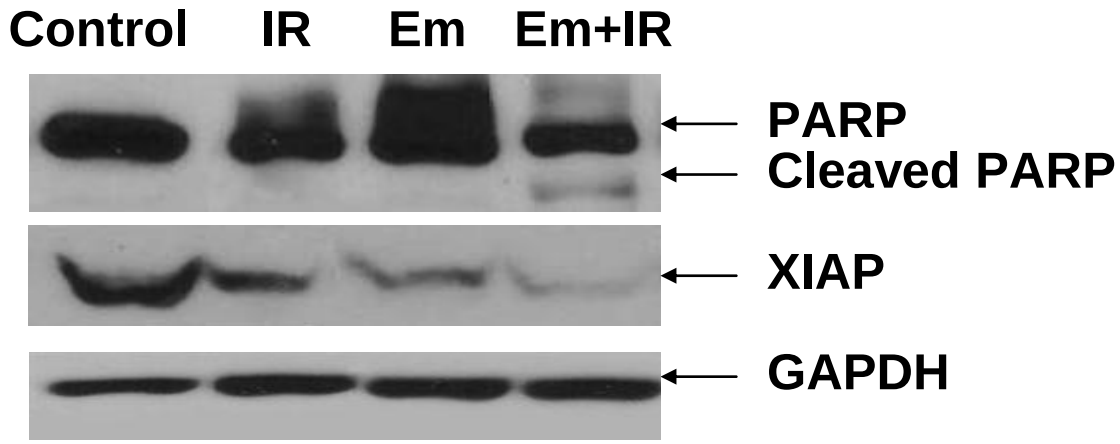

Figure 6C. Western blot analysis of tumor tissues show induction of PARP cleavage and inhibition of the anti-apoptotic protein XIAP, suggesting casepase-dependent apoptosis *in vivo*. Whole cell lysates (50 μg) of tumor tissues were probed with anti-PARP and anti-XIAP antibody. GAPDH was used as a loading control.

Supplemental Figures

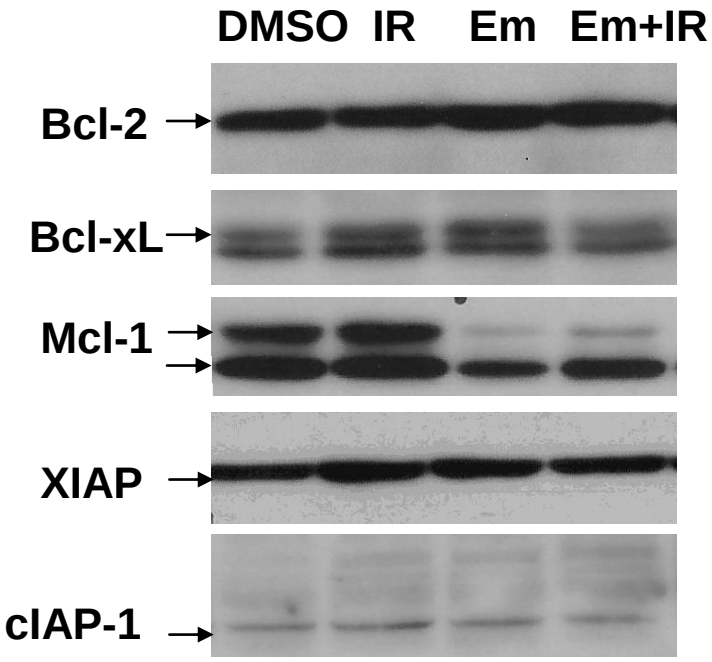

Supplemental Figure 1. Expression of anti-apoptotic proteins after Em and IR treatment *in vitro*. Samples in Figure 3D were probed with antibodies against Bcl-2 (Santa Cruz), Bcl-xL (BD), Mcl-1 (Santa Cruz), XIAP (BD) and cIAP-1 (Santa Cruz).

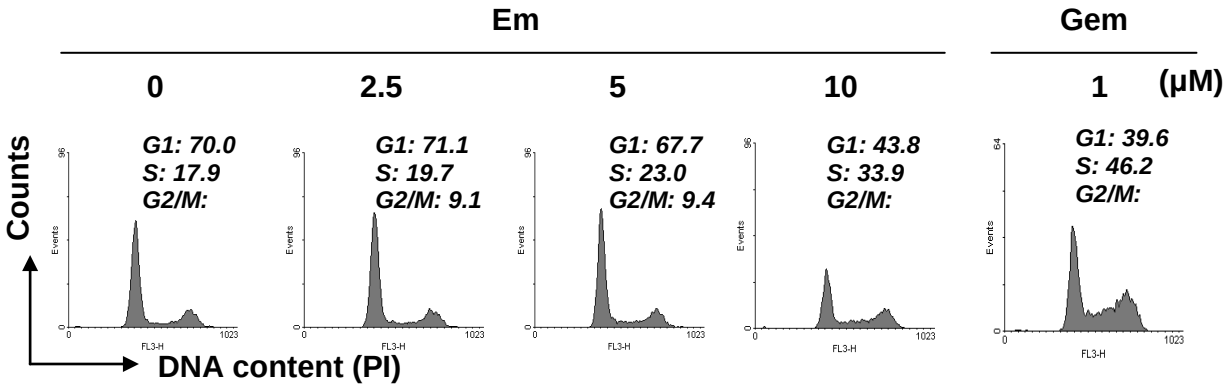

Supplemental Figure 2A. Embelin (Em) induced S-phase arrest in PC3 dose-dependently. PC3 cells were treated with various doses of Em for 72 h. Cell cycle was analyzed and cell population in each phase is numerically depicted. Gemcitabine (Gem) (Lilly, Indianapolis, Indiana) was used as a positive control, treating cells at a dose of 1 μM for 24 h. Data represent one of two independent experiments.

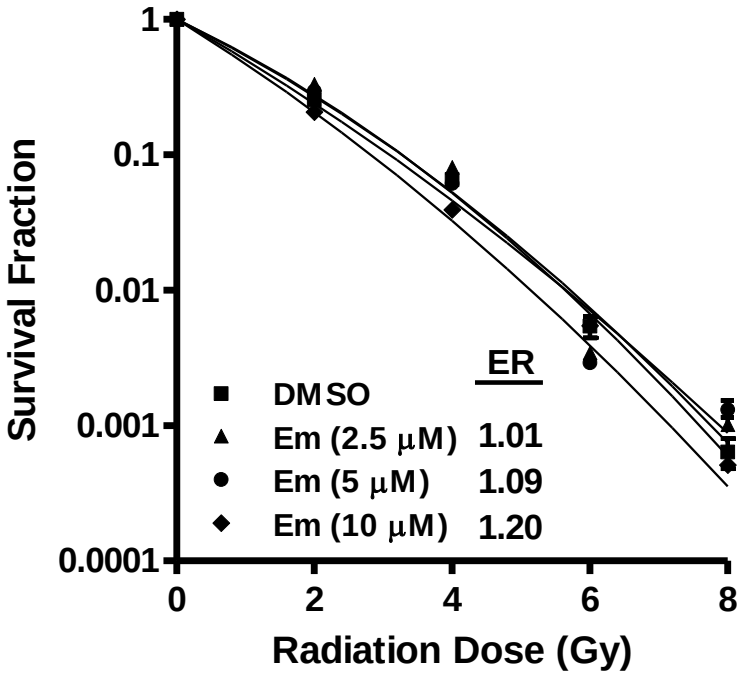

Supplemental Figure 2B. **Dose effect of embelin (Em) on radiosensitization.** Clonogenic survival curve of cells pretreated with indicated dose of Em for 72 h. Data are shown as mean ± SD (*n*=3).

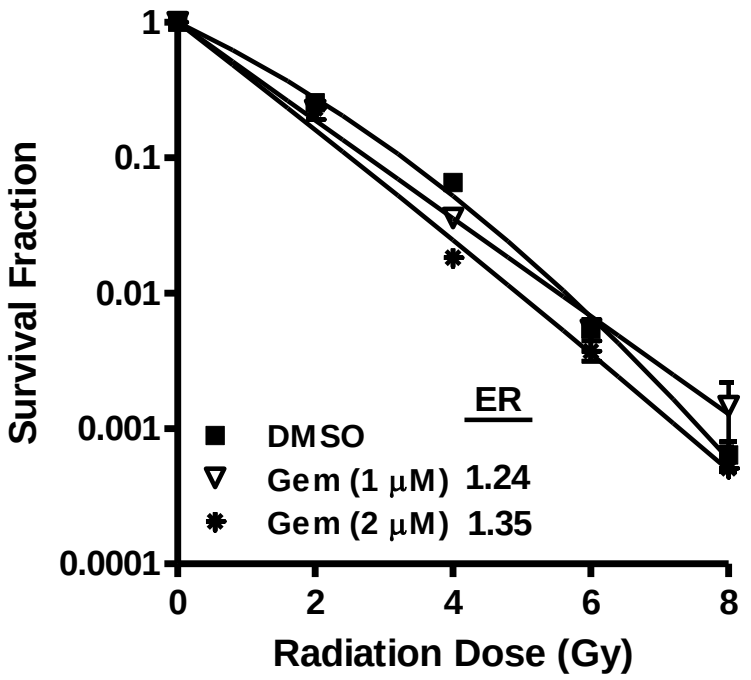

Supplemental Figure 2C. **Dose effect of gemcitabine (Gem) on radiosensitization**.

Clonogenic survival curve of cells pretreated with 1 μM and 2 μM of Gem for 24 h. Data are shown as mean ± SD (*n*=3).

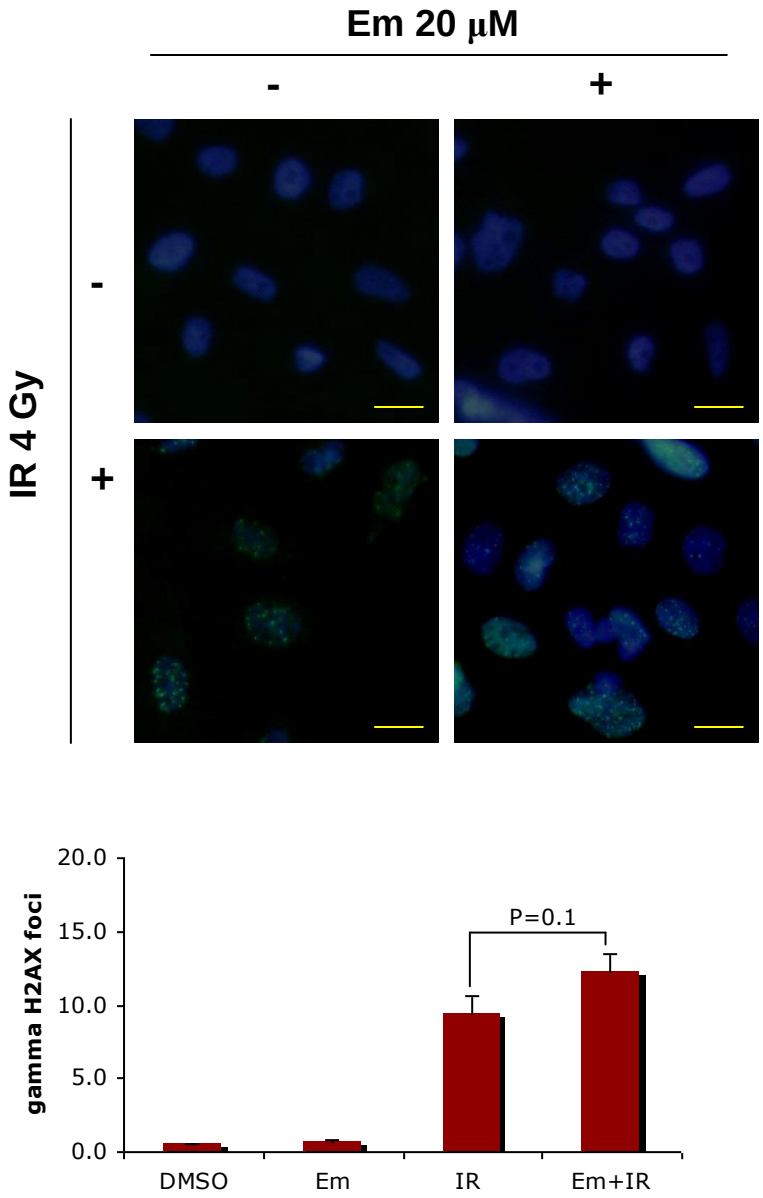

Supplemental Figure 3. Embelin (Em) treatment hardly impaired IR-induced DNA damage repair. Immunostaining of nuclear γH2AX was conducted as described previously (Dai et al, Red J 2009). γH2AX foci are shown as green fluorescent dots counterstained with DAPI. Original magnification, ×400. Fifty cells were selected randomly for foci quantification (×400). Data are shown as mean ± SD (*n*=50).

References

1. Broker LE, Kruyt FA, Giaccone G. Cell death independent of caspases: a review. Clin Cancer Res 2005; 11:3155-62.
2. Lodish HF. Molecular cell biology. 6th ed. New York: W.H. Freeman; 2008.
3. Perfettini JL, Kroemer G. Caspase activation is not death. Nat Immunol 2003; 4:308-10.
4. Gozuacik D, Kimchi A. Autophagy as a cell death and tumor suppressor mechanism. Oncogene 2004; 23:2891-906.
5. Hirsch T, Marchetti P, Susin SA, et al. The apoptosis-necrosis paradox. Apoptogenic proteases activated after mitochondrial permeability transition determine the mode of cell death. Oncogene 1997; 15:1573-81.
6. Igney FH, Krammer PH. Death and anti-death: tumour resistance to apoptosis. Nat Rev Cancer 2002; 2:277-88.
7. Los M, Burek CJ, Stroh C, Benedyk K, Hug H, Mackiewicz A. Anticancer drugs of tomorrow: apoptotic pathways as targets for drug design. Drug Discov Today 2003; 8:67-77.
8. Reed JC. Apoptosis-based therapies. Nat Rev Drug Discov 2002; 1:111-21.
9. Coffey DS. Prostate cancer. An overview of an increasing dilemma. Cancer 1993; 71:880-6.
10. Oh WK, Kantoff PW. Management of hormone refractory prostate cancer: current standards and future prospects. J Urol 1998; 160:1220-9.
11. Mike S, Harrison C, Coles B, Staffurth J, Wilt TJ, Mason MD. Chemotherapy for hormone-refractory prostate cancer. Cochrane Database Syst Rev 2006:CD005247.
12. Gentile M, Latonen L, Laiho M. Cell cycle arrest and apoptosis provoked by UV radiation-induced DNA damage are transcriptionally highly divergent responses. Nucleic Acids Res 2003; 31:4779-90.
13. Bischoff P, Altmeyer A, Dumont F. Radiosensitising agents for the radiotherapy of cancer: advances in traditional and hypoxia targeted radiosensitisers. Expert Opin Ther Pat 2009; 19:643-62.
14. Dai Y, DeSano JT, Meng Y, et al. Celastrol potentiates radiotherapy by impairment of DNA damage processing in human prostate cancer. Int J Radiat Oncol Biol Phys 2009; 74:1217-25.
15. Abbas S, Bhoumik A, Dahl R, et al. Preclinical studies of celastrol and acetyl isogambogic acid in melanoma. Clin Cancer Res 2007; 13:6769-78.
16. Nikolovska-Coleska Z, Xu L, Hu Z, et al. Discovery of embelin as a cell-permeable, small-molecular weight inhibitor of XIAP through structure-based computational screening of a traditional herbal medicine three-dimensional structure database. J Med Chem 2004; 47:2430-40.
17. Engel LW, Straus SE. Development of therapeutics: opportunities within complementary and alternative medicine. Nat Rev Drug Discov 2002; 1:229-37.
18. Riedl SJ, Renatus M, Schwarzenbacher R, et al. Structural basis for the inhibition of caspase-3 by XIAP. Cell 2001; 104:791-800.
19. Chai J, Shiozaki E, Srinivasula SM, et al. Structural basis of caspase-7 inhibition by XIAP. Cell 2001; 104:769-80.
20. Ahn KS, Sethi G, Aggarwal BB. Embelin, an inhibitor of X chromosome-linked inhibitor-of-apoptosis protein, blocks nuclear factor-kappaB (NF-kappaB) signaling

pathway leading to suppression of NF-kappaB-regulated antiapoptotic and metastatic gene products. Mol Pharmacol 2007; 71:209-19.
21. Xu L, Yang D, Wang S, et al. (-)-Gossypol enhances response to radiation therapy and results in tumor regression of human prostate cancer. Mol Cancer Ther 2005; 4:197-205.
22. Lawrence TS, Eisbruch A, McGinn CJ, Fields MT, Shewach DS. Radiosensitization by gemcitabine. Oncology (Williston Park) 1999; 13:55-60.
23. Lawrence TS, Eisbruch A, Shewach DS. Gemcitabine-mediated radiosensitization. Semin Oncol 1997; 24:S7-24-S7-8.
24. Hofer-Warbinek R, Schmid JA, Stehlik C, Binder BR, Lipp J, de Martin R. Activation of NF-kappa B by XIAP, the X chromosome-linked inhibitor of apoptosis, in endothelial cells involves TAK1. J Biol Chem 2000; 275:22064-8.
25. Altieri DC. Survivin, versatile modulation of cell division and apoptosis in cancer. Oncogene 2003; 22:8581-9.